PO Box 2345, Beijing 100023, China
www.wjgnet.com
wjg@wjgnet.com

World J Gastroenterol 2006 July 28; 12(28):4504-4510
World Journal of Gastroenterology ISSN 1007-9327

BASIC RESEARCH

Effect of rapamycin on hepatic osteodystrophy in rats with portasystemic shunting

Schalk W van der Merwe, Maria M Conradie, Robert Bond, Brenda J Olivier, Elongo Fritz, Martin Nieuwoudt, Rhena Delport, Tomas Slavik, Gert Engelbrecht, Del Kahn, Enid G Shephard, Maritha J Kotze, Nico P de Villiers, Stephen Hough

Schalk W van der Merwe, Department of Internal Medicine and Gastroenterology, Immunology, Hepatology and GI- research laboratory, University of Pretoria, South Africa
Maria M Conradie, Stephen Hough, Department of Internal Medicine and Endocrinology, University of Stellenbosch, South Africa
Robert Bond, Department of Internal Medicine and Gastroenterology1, Hepatology and GI- research laboratory, University of Pretoria, South Africa
Brenda J Olivier, Elongo Fritz, Martin Nieuwoudt, Department of Hepatology and GI- research laboratory, University of Pretoria, South Africa
Rhena Delport, Department of Chemical Pathology, University of Pretoria, South Africa
Tomas Slavik, Department of Ampath pathology, Pretoria, South Africa
Gert Engelbrecht, Del Kahn, Department of Surgery, Grootte Schuur Hospital, University of Cape Town, South Africa
Enid G Shephard, MRC Liver Research Centre, Grootte Schuur Hospital, University of Cape Town, South Africa
Maritha J Kotze, Nico P de Villiers, Department of Genecare Molecular Genetics, Christiaan Barnard Memorial Hospital, Cape Town, South Africa
Correspondence to: Dr. Schalk W van der Merwe MBChB, MMed Internal Medicine, PhD, Department of Internal Medicine and Gastroenterology, Hepatology and GI- Research laboratory University of Pretoria, PO Box 1649, Faerie Glen, Pretoria 0043, South Africa. svdm@doctors.netcare.co.za
Telephone: +27-12-6640187 Fax: +27-12-6648167
Received: 2006-01-05 Accepted: 2006-01-24

Abstract

AIM: To study if T-cell activation related to portasystemic shunting causes osteoclast-mediated bone loss through RANKL-dependent pathways. We also investigated if T-cell inhibition using rapamycin would protect against bone loss in rats.

METHODS: Portasystemic shunting was performed in male Sprague-Dawley rats and rapamycin 0.1 mg/kg was administered for 15 wk by gavage. Rats received powderized chow and supplemental feeds to prevent the effects of malnutrition on bone composition. Weight gain and growth was restored after surgery in shunted animals. At termination, biochemical parameters of bone turnover and quantitative bone histology were assessed. Markers of T-cell activation, inflammatory cytokine production, and RANKL-dependent pathways were measured. In addition, the roles of IGF-1 and hypogonadism were investigated.

RESULTS: Portasystemic shunting caused low turnover osteoporosis that was RANKL independent. Bone resorbing cytokine levels, including IL-1, IL-6 and TNFα, were not increased in serum and TNFα and RANKL expression were not upregulated in PBMC. Portasystemic shunting increased the circulating CD8+ T-cell population. Rapamycin decreased the circulating CD8+ T-cell population, increased CD8+ CD25+ T-regulatory cell population and improved all parameters of bone turnover.

CONCLUSION: Osteoporosis caused by portasystemic shunting may be partially ameliorated by rapamycin in the rat model of hepatic osteodystrophy.

Key words: Osteopenia; Liver disease; Portasystemic shunting; T-lymphocyte; Rapamycin

van der Merwe SW, Conradie MM, Bond R, Olivier BJ, Fritz E, Nieuwoudt M, Delport R, Slavik T, Engelbrecht G, Kahn D, Shephard EG, Kotze MJ, de Villiers NP, Hough S. Effect of rapamycin on hepatic osteodystrophy in rats with portasystemic shunting. *World J Gastroenterol* 2006; 12(28): 4504-4510

http://www.wjgnet.com/1007-9327/12/4504.asp

INTRODUCTION

Metabolic bone disease is a common complication of longstanding liver disease[1,2]. Mechanisms underlying bone loss remain poorly understood and may involve imbalances in bone turnover and mineralization defects. We have shown that portasystemic shunting, a complication of advanced chronic liver disease, is a major pathogenic factor causing bone loss in rats[3].

Excessive osteoclast activity, resulting in localized or generalized bone loss, occurs in various conditions associated with immune activation[4,5]. Activated T-cells express receptor activator of nuclear factor-κB ligand (RANKL) that bind to RANKL receptor on osteoclasts

activating osteoclastogenesis and bone loss[4]. This pathway produces TNFα, IL-1, IL-6, IL-7, and M-CSF all of which have been implicated in bone loss[6-10]. Blockage of RANKL by osteoprotegerin protects against bone loss[4].

The profound impact of activated T-cells on bone has been established. Osteopenia develops in ctla4$^{-/-}$ mice where T-cells are spontaneously activated, whereas bone loss fails to occur in T-cell deficient nude mice even following ovariectomy[11]. Further, RANKL expressing T-lymphocytes obtained from diseased rheumatoid arthritis joints transform healthy monocytes into osteoclast-like cells[12]. We hypothesized that endotoxin-mediated T-cell activation related to portasystemic shunting may result in osteoclast-mediated bone loss through RANKL dependent pathways.

Employing biochemical parameters of bone turnover and quantitative bone histology, this study aimed to characterize the nature of the bone disease resulting from portasystemic shunting in rats. The role of T-cell activation and inflammatory cytokine production on RANKL-dependent pathways were specifically addressed.

MATERIALS AND METHODS

Animal Experimental design

Ten-week-old male Sprague-Dawley rats weighing 200-300 g were used in all experiments. The rats were housed individually in polypropylene cages at constant room temperature (22℃ ± 2℃), humidity (55%) and 12 h light-darkness cycles. Rats were fed powderized chow (Epol, Johannesburg, South Africa) and water was given *ad libitum*. Rats received a daily 50 mL supplement (Energy 44.52 kJ, protein 0.373 g, carbohydrates 1.456 g, fat 0.373 g). Food intake was measured daily in metabolic cages during four time periods: wk 3, 9, 12 and 15. Ethics committee approval was obtained and animals were treated according to ethical guidelines of the University of Pretoria.

Group Ⅰ: n = 12 PSS. Laparotomy was performed, portal vein was ligated, transected and the distal limb anastomosed end-to-side to the IVC as previously described[3,13].

Group Ⅱ: n = 12 PSS + rapamycin. Portasystemic shunt was performed and rapamycin 0.1 mg/kg administered daily orally by gavage for 15 wk starting 1 wk after surgery. Two rats died during the study period.

Group Ⅲ: n = 12 Sham control. Laparotomy was performed and the portal vein was clamped for 8 min.

Group Ⅳ: n = 12 Sham control + rapamycin. Following laparotomy controls received rapamycin 0.1 mg/kg, orally by gavage starting 1 wk following surgery and continued for 15 wk.

Analytical methods in sera and urine

Blood and urine samples were obtained at baseline and termination and frozen at -70℃. Urine was collected from rats individually housed in metabolic cages. Routine liver tests and testosterone were performed using a Beckman CX-9 and Access auto-analyzers respectively. 25-OH Vit D was determined using scintillation counting detection[14]. Osteocalcin was measured using ELISA kit (Osteometer BioTech, Herlev, Denmark). Cytokine levels were analyzed using an ELISA kit (Biotrac, Amersham, Buckinghamshire, United Kingdom). IGF-1 was measured using an ELISA kit (DRG Inc, Mountainside, USA). Urinary deoxypyridinoline was assessed using an enzyme-labeled immunoassay (Immunolite Pyrilinks-D, Los Angeles, USA).

Liver histology

Rat liver specimens were fixed in 40 g/L buffered formaldehyde and sectioned coronally in 3 μm sections for immunoperoxidase staining utilizing antibodies to ED-1 (1:50 dilution; Serotec, Oxford, UK). Kupffer cells were counted by an experienced histopathologist in ten high power fields (Olympus BX 40, plan 40 x objective) demonstrating the most Kupffer cells. An average per high power field was then calculated.

Bone densitometry

Rats were anaesthetized and bone densitometry was performed using DEXA (DXA QDR 4500^{TM} , Hologic INC, Waltham, USA). Measurement stability was controlled daily by scanning a phantom. Whole-body and high-resolution scans of the right femur were performed at baseline and 16 wk using software for small animals (Hologic, INC, Waltham, USA).

Histomorphometry

Rats received intramuscular injections of 25 mg/kg tetracycline 13 and 3 d prior to termination. At termination the left tibia was removed, stored in 70% ethanol at 4℃, fixed in modified Millonig solution for 24 h, embedded in methylmethacrylate, sectioned at 5 μm and stained by modified Masson technique. Histomorphometric analyses were performed manually using a Merz-Schenk integrating eyepiece. Trabecular bone was analyzed excluding sections within two fields at × 250 magnification from either the growth plate or the cortices. At least 120 fields per animal were counted. Double tetracycline-labeling was assessed on 10 μm thick unstained sections cut from the proximal tibia by fluorescent microscopy using a Merz-Schenk eyepiece. Variables and units used are approved by the American Society for Bone and Mineral Research[15].

Flow cytometry

Peripheral blood obtained at termination were incubated with the following combinations of monoclonal antibodies: fluorescein isothiocyanate/phycoerythrin labeled CD4+/CD25+; CD8+/CD25+ (Immunotech, Beckman Coulter, Inc. Fullerton, USA). Analysis was performed on a Coulter Epics flow cytometer. Lymphocytes were gated on forward and side scatter. The percentage of CD3+ T-cells in the gate was deduced from the percentages for CD4+ and CD8+ T-cells.

Quantitative RT-PCR

Total RNA was extracted from PBMC using the Qiagen RNeasy kit. Aliquots of 8.5 μL were used in a RT-PCR reaction in a total volume of 20 μL (Roche, First strand cDNA synthesis kit, Mannheim, Germany).

Complementary DNA PCR primers were designed from sequences from Genbank or TIGR (Inqaba Biotech, Pretoria, South Africa). *tnfα* (Sense: 5'-atggcccagaccctcac-3', Antisense: 5'-agcacatagacggggcag-3'); *rankl* (Sense: 5'-tggaggatttttcaagctccgg-3'; Antisense: 5'-gccccaaagtacgtcgca-3') and *Gapdh* (Sense: 5'-ggcccctctggaaagct-3'; Antisense 5'-aggtggaggaatgggagt-3'). The reaction mixture consisted of cDNA (1 μL), 10 pmol of each primer, 1 μL LightCycler FastStart DNA Master SYBR Green 1 Mix (Roche, Mannheim, Germany), 500 ng BSA (Gibco, BRL, Gaithersburg, MD) and 3 mol/L $MgCl_2$ in a total volume of 10 μL. FastStart polymerase was activated and cDNA denatured by a pre-incubation of 10 min at 95℃. The template was amplified for 40 cycles of denaturation at 95℃ for 0 s, annealing at 60℃ for 8 s and extension at 72℃ for 12 s. Standard curves were generated from series diluted cDNAs and analyzed using the Light Cycler quantification software.

Analytical methods of bone calcium content

Right femurs were dried for 6 h at 60℃, then ashed for 8 h in a muffle furnace at 600℃. Bones were weighed, and the length and mid-shaft thickness measured. The femurs were dissolved in 3 mL of 6molL HCl and diluted 3000x with demineralized/de-ionized water. Calcium content was determined against a 4 point standard curve (r^2 = 0.9999), using a Perkin-Elmer 3030 atomic absorption spectrophotometer as previously described by our group[3].

Determination of 4-hydroxyproline in left femurs

Dried femurs were dissolved in 10 mL 6 mol/L HCl, at 100℃ for 24 h and centrifuged for 5 min at 4000 r/min at 4℃. n-Tetracosane ($C_{24}H_{50}$) in chloroform was added to the eluates as internal standard. The eluates were dried in nitrogen, the amino acids derivatized with N-methyl-N (*t*-butyldimethylsilyl) trifluoroacetamide and analyzed using gas chromatography as previously reported by our group[16].

Statistical analysis

Data were analyzed using SigmaStat and SigmaPlot for Windows version 4.0. Data were checked for normality and equal variance; if passed, ANOVA was performed and where failed, analysis of variance on ranks (Kruskal-Wallis) was conducted. Results are presented as means ± standard deviation. Analysis of covariance was performed to compare groups with respect to change in BMD from wk 1 to 16. Pair-wise comparisons were performed using Fisher's LSD and for between group comparison Wilcoxon rank sum test was performed. Results were considered significant at $P < 0.05$.

RESULTS

Body mass and food intake

Body mass decreased after surgery in the portasystemic shunted animals despite feeding with powderized and supplemental feeds. Weight gain was restored by wk 3 in the shunted animals and remained parallel to the control groups throughout the study (Figure 1), confirming growth in shunted animals. The rate of weight gain from wk 2 as reflected in the Pearson correlation coefficient did not differ between the shunted and control animals (Figure 1). Powderized food intake remained lower in shunted animals during the first 12 wk of the study ($P < 0.01$). The supplemental feed was consumed by all animals daily. Food intake, corrected for body mass, showed no differences between the groups with total food intake (powderized + supplemental) being higher than the recommended intake for adult laboratory rats (15 g/d). Calcium and Vit D was further supplemented in the powderized chow. By wk 15 no difference in food consumption (powderized feed) was seen (Figure 2). Body mass was still significantly lower in shunted animals at termination (Figure 1).

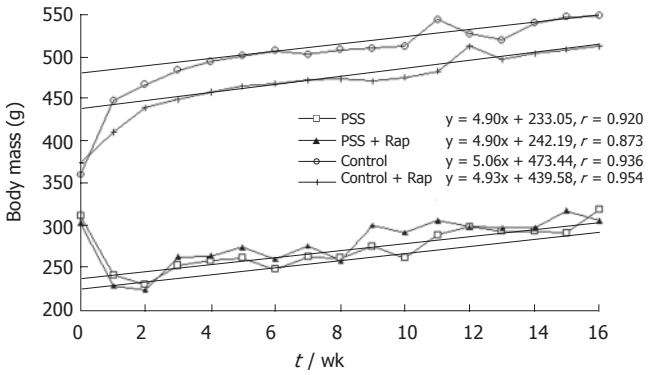

Figure 1 Body mass change per week. *r* = Pearson correlation coefficient.

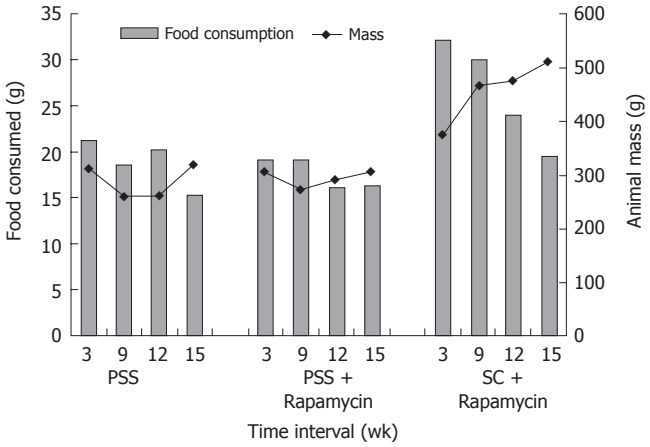

Figure 2 Food intake and body weight in PSS, PSS + rapamycin and SC + Rapamycin.

Serum and urine biochemistries

No differences were seen at baseline. Transaminase levels were elevated in shunted groups and the control group receiving rapamycin. Serum total ALP was elevated in both shunted groups and confirmed to be of hepatic origin by electrophoresis. Serum albumin, testosterone and IGF-1 levels were significantly lower in both shunted groups. 25-OH vit D levels were not different between the groups at 16 wk (Table 1). Serum osteocalcin was significantly lower in the PSS group but not different in the PSS group receiving rapamycin compared to controls (Table 1). A trend towards higher u-DPD levels was observed in

Table 1 Serum and urine biochemistries at 16 wk

	ALP (nkat)	AST (nkat)	ALT (nkat)	Albumin (g/L)	Testosterone ng/L	IGF-I μg/L	25-OH vit D ng/L	Osteocalcin ng/L	u-deoxypiridinoline (μmol/mol creatinine)
Control	2161 ± 369	1182 ± 277	940 ± 187	16.75 ± 0.71	5.41 ± 2.34	879.37 ± 245.51	25.63 ± 4.04	142.91 ± 32.9	48.8 ± 7.9
Control + rapamycin	2762 ± 389[a]	2022 ± 1152[a]	1155 ± 122[a]	15.78 ± 1.3	10.62 ± 9.1	616.02 ± 189.66	29.15 ± 8.00	147.43 ± 34.0	67.12 ± 13.6
PSS	7144 ± 2121[b]	2210 ± 741[a]	1538 ± 243[b]	15.25 ± 0.75[a]	3.55 ± 0.41[a]	290.28 ± 170.90[a]	23.89 ± 5.97	105.57 ± 38.3[a]	61.99 ± 18.7
PSS + rapamycin	8481 ± 3380[b]	3217 ± 1560[a]	1752 ± 549[a]	14.33 ± 1.22[a]	3.45 ± 0.74[b]	241.66 ± 80.58[a]	22.15 ± 5.07	119.61 ± 43.5	93.79 ± 30.6[a]

[a]$P < 0.05$ *vs* Controls; [b]$P < 0.001$ *vs* Controls.

Table 2 Bone analysis at 16 wk

	Whole body BMD mg/cm^2	High resolution BMD mg/cm^2	Femur length (mm)	Mid-shaft thickness (mm)	Femur mass (g)/kg body mass	Ca^{2+} mg/g bone	Hyp/g bone
Control (n = 12)	211.7 ± 9	379.7 ± 46	42.8 ± 1.1	4.7 ± 0.3	1.49 ± 0.1	260 ± 7	3576 ± 1980
Control + rapamycin (n = 12)	210.0 ± 8	377.2 ± 43	42.8 ± 1.3	4.7 ± 0.3	1.53 ± 0.1	258 ± 9	6104 ± 1600[a]
PSS (n = 11)	201.9 ± 8[a]	309.3 ± 63[a]	36.6 ± 0.6[b]	4.1 ± 0.3[a]	1.80 ± 0.2[a]	289 ± 5[b]	2038 ± 878
PSS + Rapamycin (n = 10)	210.5 ± 17	334. ± 64	37.3 ± 1[b]	3.8 ± 0.3[b]	1.81 ± 1.37[b]	297 ± 9[b]	5489 ± 1250[a]

[a]$P < 0.05$ *vs* Controls; [b]$P < 0.001$ *vs* Controls.

Table 3 Quantitative histomorphometry

	Osteoid volume, OV/BV (%)	Relative osteoid volume, OV/TV (%)	Osteoid surface, OS/BS (%)	Osteoid thickness, O.Th (μm)	Osteoblast appositional rate, OAR (μm/d)	Mineralization lag time, MLT (d)	Eroded surfaces, ES/BS (%)	Osteoclastic surfaces, OcS/BS (%)
Control	1.26 ± 0.24	0.15 ± 0.04	8.94 ± 1.27	5.67 ± 0.65	1.03 ± 0.09	5.61 ± 1.08	5.63 ± 0.55	1.07 ± 0.20
Control + Rapamycin	1.34 ± 0.38	0.19 ± 0.06	10.44 ± 1.86	5.30 ± 0.93	1.05 ± 0.08	5.06 ± 1.25	6.35 ± 0.81	1.42 ± 0.24
PSS	3.69 ± 1.43	0.66 ± 0.32	17.48 ± 4.96	8.00 ± 1.32	0.85 ± 0.86	19.7 ± 5.07[a]	3.62 ± 0.63[a]	0.97 ± 0.28
PSS + Rapamycin	1.33 ± 0.19	0.15 ± 0.02	10.05 ± 1.53	5.72 ± 0.86	0.95 ± 0.11	11.02 ± 1.99	4.40 ± 0.62	0.94 ± 0.19

[a]$P < 0.05$ *vs* Controls.

shunted animals compared to control animals. Significantly higher u-DPD levels were seen in control animals receiving rapamycin.

DEXA, bone mass and composition

Mean whole body and femoral BMD were comparable at baseline. At 16 wk whole body and high resolution femoral BMD were significantly lower in portasystemic animals compared to controls (Table 2). BMD in PSS receiving rapamycin did not differ from controls. The change in BMD from baseline to wk 16 using pair-wise comparisons showed that the increase in BMD in the shunted group (group I) was significantly lower compared to the control group ($P = 0.006$). The increase in BMD in the PSS receiving rapamycin was comparable to controls ($P = 0.07$). Shunted animals had lower body mass, femoral length and thickness (Table 2). Femur mass, expressed as a function of body mass, was increased in PSS. Femoral calcium content, expressed as a function of femoral mass (mg Ca^{2+}/mg femur), was not decreased in shunted animals, excluding significant osteomalacia. Femoral hydroxyproline levels tended to be lower in the PSS group compared with controls (Table 2). Unexpectedly, shunted and control rats receiving rapamycin had significantly higher femoral hydroxyproline.

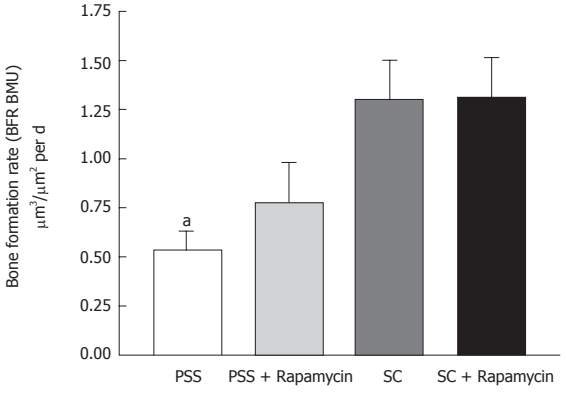

Figure 3 Effect of portasystemic shunting and rapamycin administration on dynamic bone formation in the proximal tibias of rats. BFRBMU = Bone formation rate at the level of the basic multi-cellular unit. (mean ± SE. [a]$P < 0.05$ *vs* SC).

Quantitative Histomorphometry

Osteoid volumes and surfaces, and mean osteoid seam thickness, was higher in the PSS compared with control animals (Table 3). Bone formation was decreased in PSS rats (Figure 3). Mineralization of newly formed osteoid,

Table 4 Cytokine levels, T-lymphocyte subsets and Kupffer cell populations at 16 wk

	IL-1 (ng/L)	IL-6 (ng/L)	TNFa (ng/L)	%CD3+	%CD4+	%CD8+	Ratio CD4+: CD8+	%CD4+ expressing CD25	%CD8+ expressing CD25	Kupffer cells /10 high power fields
Control	22.28 ± 4.39	0	13.6 ± 2.73	74.05 ± 5.49	43.15 ± 3.93	30.9 ± 7.05	1.4	7.96 ± 2.99[d]	10.62 ± 2.64[f]	46.26 ± 7.95
Control + rapamycin	25.86 ± 8.71	0	14.84 ± 2.35	73.34 ± 7.73	47.86 ± 8.31	25.48 ± 6.4	1.8	15.54 ± 9.5[d]	17.9 ± 13.87[f]	40.3 ± 8.46
PSS	22.23 ± 5.12	0.025 ± 0.045	26.15 ± 45.97	93.4 ± 7.97[a]	58.96 ± 9.02	34.47 ± 6.59[b]	1.6	5.38 ± 2.47[c]	6.05 ± 1.99[e]	43.45 ± 8.13
PSS + Rapamycin	26.12 ± 6.21	0.011 ± 0.033	15.5 ± 11.83	73.19 ± 5.66	56.78 ± 5.60	18.39 ± 5.73[b]	3.1	11.38 ± 6.96[c]	19.10 ± 14.58[e]	44.95 ± 9.16

%CD3 + T cells PSS *vs* controls [b]$P < 0.001$ *vs* Controls; %CD8+ T cells PSS *vs* PSS + Rapamycin [d]$P < 0.001$; %CD4 + CD25 + T cells PSS *vs* PSS + Rapamycin [f]$P < 0.001$; %CD4 + CD25 + T cells Control *vs* Control + Rapamycin [h]$P < 0.001$; %CD8 + CD25 + T cells PSS *vs* PSS + Rapamycin [i]$P < 0.001$; %CD8 + CD25 + T cells Control *vs* Control + Rapamycin [k]$P < 0.001$.

reflected in the mineralization lag time, was significantly delayed in PSS rats, accounting for the accumulation of osteoid in these animals (Table 3). Bone resorption over 16 wk, as reflected in the total eroded surfaces, was significantly decreased in PSS animals, although active osteoclastic resorption at the time of sacrifice was comparable among groups (Table 3). Bone turnover in shunted animals was increased by rapamycin as evidenced by increase bone formation and resorption. Osteoid accumulation and the mineralization defect induced by shunting were largely normalized by rapamycin (Table 3).

T-cells, cytokine levels and tnfα and rankl expression

PSS increased the percentage of circulating CD3+ lymphocytes by 1.3 fold ($P < 0.001$) above that for control rats (Table 4). Rapamycin treatment of PSS rats returned the CD3+ T-cell population to that of control rats with an altered ratio of CD4+ to CD8+ T-cells of 3:1. No alteration occurred in either the size of the CD3+ population or the normal ratio of CD4+ to CD8+ T-cells in rapamycin treated control rats (Table 4). PSS did not affect the normal CD4+ or CD8+ T-cells fractions expressing CD25. There was a significant increase ($P < 0.001$) in the percentage of CD4+ and CD8+ T-cells expressing CD25 with rapamycin treatment in both PSS and control rats (Table 4). Serum levels of IL-1, IL-6 and TNFα were similar in all groups (Table 4). RT-PCR showed that TNFα gene expression in shunted and control animals was comparable. RANKL-expression was significantly lower in PSS animals.

DISCUSSION

We previously investigated the contribution of parenchymal inflammation, portal hypertension and portasystemic shunting to the development of metabolic bone disease using rat models. Only portasystemic shunting caused significant bone loss[3]. The present study aimed to delineate the immune responses associated with portasystemic shunting and how this may influence bone loss in the rat. Further, the profound effect of activated T-cells on bone turnover has been well established [11,12]. We set out to study the effect of T-cell inhibition using rapamycin, not shown to have adverse effects on bone composition (in contrast to cyclosporin and tacrolimus), on biochemical and histological bone parameters in rats following portasystemic shunting.

The present study confirmed the adverse effect of portasystemic shunting on skeletal integrity as evident by a significant decrease in whole-body and femoral BMD. Quantitative bone histology documented hyperosteoidosis and an increased mineralization lag time in shunted animals, suggesting a degree of impaired mineralization. Histological evidence of frank osteomalacia was absent. Serum 25-OH vitamin D levels and femoral calcium content were comparable between shunted and control animals, and ALP iso-enzymes in shunted animals originated from liver not bone, supporting the histological evidence that the low BMD observed in shunted animals was mainly the result of osteoporosis.

Femur mass per 100 g body mass was higher in shunted rats compared to controls. Trabecular bone loss is known to occur earlier and more extensive compared to cortical bone loss due to the large surface area available for resorption. The apparent discrepancy between the rise in femur mass per 100 g of body mass in portasystemic shunted animals may be explained by lean body mass being lost earlier and more rapidly than cortical bone mass so that a lag in cortical bone loss gives rise to an apparent increase in bone mass relative to body mass. Low-turnover osteoporosis may occur due to protein-energy malnutrition[17]. IGF-1 and testosterone levels were decreased in the shunted rats. Malnutrition[18] and liver disease[19] have been associated with decreased circulating levels of IGF-1. Low testosterone levels have been previously documented in portasystemic shunted rats[20] with osteoporosis[3]. IGF-1 has previously been implicated in bone loss in chronic liver disease[21,22].

It is not possible to exclude that malnutrition contributed to bone loss in shunted rats. Malnutrition is associated with advanced liver disease although muscle wasting independent of malnutrition may be a feature of liver cirrhosis[23]. Reduced spontaneous locomotor activity due to altered histaminergic neurotransmission can reduce food intake in shunted rats[24]. We could, however, document that food intake in the shunted animals met the nutritional requirements calculated for their body weights during four time periods. However, despite restoring growth and weight gain (Figure 1), osteoporosis still developed in the portasystemic shunted rats. This improved feeding protocol may explain the differences observed in the present study compared to

our previous study[3] In our previous study weight loss was observed throughout the study period and TNFα levels were increased and vitamin D levels decreased in shunted animals. In the current study TNFα and vitamin D levels did not differ from the control animals suggesting a stable model due to improved feeding.

An important observation in the study was that portasystemic shunted animals receiving rapamycin had increased bone formation, whole body and high resolution BMD, as well as increased osteocalcin levels in serum and hydroxyproline content in femurs, compared to shunted animals not receiving rapamycin. These positive changes on bone turnover variables occurred despite lower body mass, IGF-1 and testosterone levels compared to controls. This finding further suggests that malnutrition and decreased IGF-1 and low testosterone levels can only partially explain osteoporosis observed in shunting.

Pro-inflammatory cytokines like IL-1, IL-6, TNFα and RANKL are known to activate osteoclastogenesis and cause high-turnover osteoporosis[9-11,25]. Serum levels of IL-1, IL-6 and TNFα, and *tnf*-α and *rankl* gene expression in PBMC, were not increased in shunted rats. Instead, osteocalcin, a marker of bone formation, was significantly decreased and quantitative histomorphometry showed impaired bone formation, suggesting low-turnover bone disease in shunted rats. Collectively, these observations suggest that the pro-inflammatory cytokines studied, are not responsible for bone loss in portasystemic shunting.

Rapamycin decreased the circulating CD8+ T-cell population in PSS rats. Lymphocyte proliferation inhibition by rapamycin is known to be dependent on the activation pathway of the proliferative signal with CD8+ T-cell proliferation being more affected than CD4+ T-cell proliferation[26-28]. The effect of rapamycin on the CD8+ T-cell population in PSS rats indicate that these cells are more activated than CD4+ T-cells.

Expression of the CD25 marker in this study does not appear to reflect cellular activation. There was no difference between the control group and PSS group with respect to fraction of CD4+ or CD8+ T-cells expressing the CD25 marker, suggesting that the cells expressing CD25 belong to a population of regulatory T-cells (Treg cells). Treg cells in mice and humans are associated with a restriction of most immune responses[29]. No documentation of such cell populations in rats has been made. Rapamycin increased the percentage of CD4+ and CD8+ T-cells expressing CD25 for both normal and shunted rats. This has been proposed to be a component of the immunosuppressive properties of rapamycin[30]. Although not much is known of the function of the CD8+CD25+ T-cell population in rodents, this population in humans has similar immunoregulatory characteristics to the CD4+CD25+ T-cell population[31,32]. Murine studies indicate an inability of CD8+CD25+ T-cells to induce osteoclast differentiation[33]. In shunted rats where the fraction of these cells was increased by rapamycin, increased bone formation was observed. An increase in this population of CD8+ T-cells by rapamycin in normal rats also increased hydroxyproline levels in femurs.

The overall changes in the lymphocyte population seen with rapamycin treatment of shunted rats are associated with an increase in bone formation, whole body and high resolution BMD as well as higher circulating levels of osteocalcin and femoral hydroxyproline content. Although IL-1, IL-6, TNFα and RANKL do not appear to be involved in portasystemic shunting associated osteopenia, other cytokines that are modulated by rapamycin may be implicated. IFNγ suppresses osteoclast activity while macrophage production of IL-12, a major stimulator of lymphocyte IFNγ production is upregulated by rapamycin. T-cell production of IFNγ via an IL-12 mechanism may be important in the bone protection observed in rapamycin treated animals[34,35]. An alternative explanation whereby rapamycin may increase bone formation is through mTOR a member of the phosphoinositide 3-kinase related kinase (PIKK) family, which plays a critical role in transducing proliferative signals mediated through the PI3K/Akt signalling pathway[36]. The mTOR gene is expressed in osteoblasts[37,38] and rapamycin has been shown to up-regulate growth factors like BMP-4 and latent TGF-β binding protein in certain cancer cell lines[39]. This may present an additional pathway by which bone formation is stimulated by rapamycin.

In conclusion, we hypothesized that portasystemic shunting would result in T-cell activation, cytokine mediated osteoclastogenesis and high-turnover osteoporosis. Instead, we documented low-turnover osteoporosis, which was partially ameliorated by rapamycin. A better understanding of the direct mechanisms of rapamycin on bone is required.

ACKNOWLEDGMENTS

The contributions of Ms. Anna Biscardi, department of Orthopaedic surgery and MRC Mineral metabolism unit, University of the Witwatersrand for bone densitometry work; Professor Christine Schnitzler and Professor Johan Fevery for evaluation of the manuscript and for valuable comments made; also the contributions of the Mr. Mario Smuts and his team at the Biomedical Research facility of the University of Pretoria for the animal preparation, post-operative care and daily dosing of Rapamycin.

REFERENCES

1 **Diamond T**, Stiel D, Lunzer M, Wilkinson M, Roche J, Posen S. Osteoporosis and skeletal fractures in chronic liver disease. *Gut* 1990; **31**: 82-87

2 **Leslie WD**, Bernstein CN, Leboff MS. AGA technical review on osteoporosis in hepatic disorders. *Gastroenterology* 2003; **125**: 941-966

3 **van der Merwe SW**, van den Bogaerde JB, Goosen C, Maree FF, Milner RJ, Schnitzler CM, Biscardi A, Mesquita JM, Engelbrecht G, Kahn D, Fevery J. Hepatic osteodystrophy in rats results mainly from portasystemic shunting. *Gut* 2003; **52**: 580-585

4 **Kong YY**, Feige U, Sarosi I, Bolon B, Tafuri A, Morony S, Capparelli C, Li J, Elliott R, McCabe S, Wong T, Campagnuolo G, Moran E, Bogoch ER, Van G, Nguyen LT, Ohashi PS, Lacey DL, Fish E, Boyle WJ, Penninger JM. Activated T cells regulate bone loss and joint destruction in adjuvant arthritis through osteoprotegerin ligand. *Nature* 1999; **402**: 304-309

5 **Saito K**, Ohara N, Hotokezaka H, Fukumoto S, Yuasa K, Naito M, Fujiwara T, Nakayama K. Infection-induced up-regulation of the costimulatory molecule 4-1BB in osteoblastic cells and its inhibitory effect on M-CSF/RANKL-induced in vitro osteo-

clastogenesis. *J Biol Chem* 2004; **279**: 13555-13563
6 **Cenci S**, Toraldo G, Weitzmann MN, Roggia C, Gao Y, Qian WP, Sierra O, Pacifici R. Estrogen deficiency induces bone loss by increasing T cell proliferation and lifespan through IFN-gamma-induced class II transactivator. *Proc Natl Acad Sci USA* 2003; **100**: 10405-10410
7 **Toraldo G**, Roggia C, Qian WP, Pacifici R, Weitzmann MN. IL-7 induces bone loss in vivo by induction of receptor activator of nuclear factor kappa B ligand and tumor necrosis factor alpha from T cells. *Proc Natl Acad Sci USA* 2003; **100**: 125-130
8 **Boyle WJ**, Simonet WS, Lacey DL. Osteoclast differentiation and activation. *Nature* 2003; **423**: 337-342
9 **Livshits G**, Pantsulaia I, Trofimov S, Kobyliansky E. Genetic influences on the circulating cytokines involved in osteoclastogenesis. *J Med Genet* 2004; **41**: e76
10 **Weitzmann MN**, Cenci S, Rifas L, Brown C, Pacifici R. Interleukin-7 stimulates osteoclast formation by up-regulating the T-cell production of soluble osteoclastogenic cytokines. *Blood* 2000; **96**: 1873-1878
11 **Roggia C**, Tamone C, Cenci S, Pacifici R, Isaia GC. Role of TNF-alpha producing T-cells in bone loss induced by estrogen deficiency. *Minerva Med* 2004; **95**: 125-132
12 **Kotake S**, Udagawa N, Hakoda M, Mogi M, Yano K, Tsuda E, Takahashi K, Furuya T, Ishiyama S, Kim KJ, Saito S, Nishikawa T, Takahashi N, Togari A, Tomatsu T, Suda T, Kamatani N. Activated human T cells directly induce osteoclastogenesis from human monocytes: possible role of T cells in bone destruction in rheumatoid arthritis patients. *Arthritis Rheum* 2001; **44**: 1003-1012
13 **Benjamin IS**, Ryan CJ, Engelbrecht GH, Campbell JA, van Hoorn-Hickman R, Blumgart LH. Portacaval transposition in the rat: definition of a valuable model for hepatic research. *Hepatology* 1984; **4**: 704-708
14 **Shephard GS**, Carlini SM, Hanekom C, Labadarios D. Analysis of 25-hydroxyvitamin D in plasma using solid phase extraction. *Clin Chim Acta* 1987; **167**: 231-236
15 **Parfitt AM**, Drezner MK, Glorieux FH, Kanis JA, Malluche H, Meunier PJ, Ott SM, Recker RR. Bone histomorphometry: standardization of nomenclature, symbols, and units. Report of the ASBMR Histomorphometry Nomenclature Committee. *J Bone Miner Res* 1987; **2**: 595-610
16 **Delport M**, Maas S, van der Merwe SW, Laurens JB. Quantitation of hydroxyproline in bone by gas chromatography-mass spectrometry. *J Chromatogr B Analyt Technol Biomed Life Sci* 2004; **804**: 345-351
17 **Bonjour JP**, Ammann P, Chevalley T, Rizzoli R. Protein intake and bone growth. *Can J Appl Physiol* 2001; **26** Suppl: S153-166
18 **Goya L**, Garcia-Segura LM, Ramos S, Pascual-Leone AM, Argente J, Martin MA, Chowen JA. Interaction between malnutrition and ovarian hormones on the systemic IGF-I axis. *Eur J Endocrinol* 2002; **147**: 417-424
19 **Vyzantiadis T**, Theodoridou S, Giouleme O, Harsoulis P, Evgenidis N, Vyzantiadis A. Serum concentrations of insulin-like growth factor-I (IGF-I) in patients with liver cirrhosis. *Hepatogastroenterology* 2003; **50**: 814-816
20 **Van Thiel DH**, Gavaler JS, Cobb CF, McClain CJ. An evaluation of the respective roles of portosystemic shunting and portal hypertension in rats upon the production of gonadal dysfunction in cirrhosis. *Gastroenterology* 1983; **85**: 154-159
21 **Cemborain A**, Castilla-Cortazar I, Garcia M, Muguerza B, Delgado G, Diaz-Sanchez M, Picardi A. Effects of IGF-I treatment on osteopenia in rats with advanced liver cirrhosis. *J Physiol Biochem* 2000; **56**: 91-99
22 **Cemborain A**, Castilla-Cortazar I, Garcia M, Quiroga J, Muguerza B, Picardi A, Santidrian S, Prieto J. Osteopenia in rats with liver cirrhosis: beneficial effects of IGF-I treatment. *J Hepatol* 1998; **28**: 122-131
23 **Scharf JG**, Schmitz F, Frystyk J, Skjaerbaek C, Moesus H, Blum WF, Ramadori G, Hartmann H. Insulin-like growth factor-I serum concentrations and patterns of insulin-like growth factor binding proteins in patients with chronic liver disease. *J Hepatol* 1996; **25**: 689-699
24 **Lozeva V**, Valjakka A, Lecklin A, Olkkonen H, Hippelainen M, Itkonen M, Plumed C, Tuomisto L. Effects of the histamine H(1) receptor blocker, pyrilamine, on spontaneous locomotor activity of rats with long-term portacaval anastomosis. *Hepatology* 2000; **31**: 336-344
25 **Troen BR**. Molecular mechanisms underlying osteoclast formation and activation. *Exp Gerontol* 2003; **38**: 605-614
26 **Blazar BR**, Taylor PA, Panoskaltsis-Mortari A, Vallera DA. Rapamycin inhibits the generation of graft-versus-host disease- and graft-versus-leukemia-causing T cells by interfering with the production of Th1 or Th1 cytotoxic cytokines. *J Immunol* 1998; *160*: 5355-5365
27 **Vu MD**, Amanullah F, Li Y, Demirci G, Sayegh MH, Li XC. Different costimulatory and growth factor requirements for CD4+ and CD8+ T cell-mediated rejection. *J Immunol* 2004; **173**: 214-221
28 **Barten MJ**, Streit F, Boeger M, Dhein S, Tarnok A, Shipkova M, Armstrong VW, Mohr FW, Oellerich M, Gummert JF. Synergistic effects of sirolimus with cyclosporine and tacrolimus: analysis of immunosuppression on lymphocyte proliferation and activation in rat whole blood. *Transplantation* 2004; **77**: 1154-1162
29 **Sakaguchi S**. Naturally arising CD4+ regulatory t cells for immunologic self-tolerance and negative control of immune responses. *Annu Rev Immunol* 2004; **22**: 531-562
30 **Tian L**, Lu L, Yuan Z, Lamb JR, Tam PK. Acceleration of apoptosis in CD4+CD8+ thymocytes by rapamycin accompanied by increased CD4+CD25+ T cells in the periphery. *Transplantation* 2004; **77**: 183-189
31 **Cosmi L**, Liotta F, Lazzeri E, Francalanci M, Angeli R, Mazzinghi B, Santarlasci V, Manetti R, Vanini V, Romagnani P, Maggi E, Romagnani S, Annunziato F. Human CD8+CD25+ thymocytes share phenotypic and functional features with CD4+CD25+ regulatory thymocytes. *Blood* 2003; **102**: 4107-4114
32 **Xystrakis E**, Dejean AS, Bernard I, Druet P, Liblau R, Gonzalez-Dunia D, Saoudi A. Identification of a novel natural regulatory CD8 T-cell subset and analysis of its mechanism of regulation. *Blood* 2004; **104**: 3294-3301
33 **Choi Y**, Woo KM, Ko SH, Lee YJ, Park SJ, Kim HM, Kwon BS. Osteoclastogenesis is enhanced by activated B cells but suppressed by activated CD8(+) T cells. *Eur J Immunol* 2001; **31**: 2179-2188
34 **Takayanagi H**, Ogasawara K, Hida S, Chiba T, Murata S, Sato K, Takaoka A, Yokochi T, Oda H, Tanaka K, Nakamura K, Taniguchi T. T-cell-mediated regulation of osteoclastogenesis by signalling cross-talk between RANKL and IFN-gamma. *Nature* 2000; **408**: 600-605
35 **Tsiavou A**, Degiannis D, Hatziagelaki E, Koniavitou K, Raptis S. Flow cytometric detection of intracellular IL-12 release: in vitro effect of widely used immunosuppressants. *Int Immunopharmacol* 2002; **2**: 1713-1720
36 **Glantschnig H**, Fisher JE, Wesolowski G, Rodan GA, Reszka AA. M-CSF, TNFalpha and RANK ligand promote osteoclast survival by signaling through mTOR/S6 kinase. *Cell Death Differ* 2003; **10**: 1165-1177
37 **Tokuda H**, Hatakeyama D, Shibata T, Akamatsu S, Oiso Y, Kozawa O. p38 MAP kinase regulates BMP-4-stimulated VEGF synthesis via p70 S6 kinase in osteoblasts. *Am J Physiol Endocrinol Metab* 2003; **284**: E1202-1209
38 **Kozawa O**, Matsuno H, Uematsu T. Involvement of p70 S6 kinase in bone morphogenetic protein signaling: vascular endothelial growth factor synthesis by bone morphogenetic protein-4 in osteoblasts. *J Cell Biochem* 2001; **81**: 430-436
39 **van der Poel HG**, Hanrahan C, Zhong H, Simons JW. Rapamycin induces Smad activity in prostate cancer cell lines. *Urol Res* 2003; **30**: 380-386

S- Editor Pan BR **L- Editor** Worthley DL **E- Editor** Ma WH